

# Electrochemistry in Near-Critical and Supercritical Fluids. 4. Nitrogen Heterocycles, Nitrobenzene, and Solvated Electrons in Ammonia at Temperatures to 150 °C

Richard M. Crooks and Allen J. Bard\*

Department of Chemistry, University of Texas, Austin, Texas 78712 (Received: September 10, 1986)

The electrochemistry of pyrazine, quinoxaline, phenazine, and solvated electrons in near-critical and supercritical ammonia was investigated by cyclic voltammetry and chronoamperometry and compared to that in liquid ammonia at  $-40\text{ }^{\circ}\text{C}$ . The reductions of pyrazine, quinoxaline, and phenazine at room temperature, and in the supercritical fluid (SCF), occur reversibly or quasi-reversibly and result in stable products (anion radicals or dianions) on the voltammetric time scale. The electrochemistry of nitrobenzene was investigated in the presence of water, and reactions of the dianion at higher temperature, similar to those previously reported at  $-40\text{ }^{\circ}\text{C}$ , were observed. The diffusion coefficient of the four aromatics increased by an order of magnitude between  $-40\text{ }^{\circ}\text{C}$  and  $+150\text{ }^{\circ}\text{C}$ , in agreement with the Stokes-Einstein relationship over the temperature range studied. Solvated electrons were electrochemically generated in the supercritical fluid and found to be stable on the voltammetric time scale. The thermodynamics of electrode reactions in the SCF is discussed, and the apparatus for performing electrochemistry in the SCF is described.

## Introduction

Our laboratory has been engaged in extracting quantitative electrochemical information from species in supercritical fluids (SCF).<sup>1,2</sup> In this article we report the cyclic voltammetry and chronoamperometry of a series of aza aromatic compounds (pyrazine, quinoxaline, and phenazine) and nitrobenzene and the generation of solvated electrons in near-critical and supercritical ammonia. We have investigated the thermodynamics, mass transport, and chemical stability of these species and show, for the first time, electrochemistry of organic species in supercritical ammonia. Supercritical fluids have interesting solvating characteristics and provide greatly increased mass-transfer rates; the results reported here, to our knowledge, represent the highest rates of diffusion to an electrode in an electrochemical system. We also describe details about the experimental apparatus required for high-pressure/high-temperature electrochemistry in ammonia.

The useful properties of near-critical and supercritical fluids are temperature and pressure induced. As the temperature of a liquid is increased along its characteristic vapor pressure curve, the thermodynamic properties change in a predictable way; for example, the dielectric constant ( $\epsilon$ ) and density ( $\rho$ ) fall due to a loss in orientation polarization brought about by thermal randomization. The physical properties of the vapor change in an opposite way: as the temperature increases,  $\epsilon$  and  $\rho$  increase. At the critical temperature,  $T_c$ , the thermodynamic natures of the vapor and liquid phases become indistinguishable and therefore cannot support a phase boundary. Above  $T_c$ , the thermodynamic properties of the SCF become very sensitive to pressure variations, since the fluids are readily compressed. For example,  $\epsilon$  and  $\rho$  are continuously variable over a broad range with relatively small changes of pressure. Since these parameters are in large part responsible for solvation characteristics, the primary goal of SCF research has been to understand and utilize the tunable solvating power of these fluids. The thermodynamic and experimental particulars of polar SCF have been reviewed elsewhere.<sup>3a,6</sup>

The range of temperatures we used for electrochemical studies in ammonia and the physical properties of  $\text{NH}_3$  at these temperatures are given in Table I.<sup>3-5</sup> In principle, and  $\epsilon$ ,  $\rho$ , or viscosity

TABLE I: Properties of Ammonia

	temperature domain			
	low	room	critical	working
$T, \text{ }^{\circ}\text{C}$	-40	25	133	150
$P, \text{ bar}$	0.7	9.5	112	285
$\rho, \text{ g/cm}^3$	0.69	0.60	0.24	0.43
$\epsilon$	23	17	3-4	8
$\eta, \text{ cP}$	0.28	0.15	0.024	0.054

( $\eta$ ) is achievable for fluids above  $T_c$ ; however, present experimental limitations have restricted our study to roughly the range of values shown. The motivation for using ammonia as an electrochemical solvent has been either to provide an aprotic environment to study radical anions or other unstable intermediates or to take advantage of the low working temperature of liquid ammonia to slow the kinetics of chemical reactions.<sup>7</sup> We show here that the low acidity of ammonia is not changed greatly above  $T_c$  and, therefore, that ammonia remains a useful medium for the study of such phenomena, even under high-temperature and high-pressure conditions. We have been able to study the same types of reactions which have previously been studied at low temperature, but with far more control over the nature of the solvent. Reliable measurements of electrode processes and diffusion above room temperature, such as those reported here, will provide heretofore unavailable thermodynamic information about electron-transfer reactions and the nature of the solvation and structure within the

(5) (a) Gronier, W. S.; Thodos, G. *J. Chem. Eng. Data* **1979**, *6*, 240-244. (b) Carmichael, L. T.; Reamer, H. H.; Sage, B. H. *J. Chem. Eng. Data* **1963**, *8*, 400-404.

(6) (a) Franck, E. U.; Deul, R. *Faraday Discuss. Chem. Soc.* **1979**, *191-198*. (b) Cobble, J. W.; Murray, R. C., Jr. *Faraday Discuss. Chem. Soc.* **1977**, *144-149*. (c) Hills, G. J.; Ovenden, P. J. In *Advances in Electrochemistry and Electrochemical Engineering*; Delahay, P., Tobias, C., Eds.; Wiley: New York, 1965; pp 185-247. (d) Franck, E. U. *Ber. Bunsenges. Phys. Chem.* **1984**, *88*, 820-825. (e) MacDonald, D. D. In *Modern Aspects of Electrochemistry*; Conway, B. E., Bockris, J. O'M., Eds.; Plenum: New York, 1975; Vol. 11, pp 141-197. (f) Kobe, K. A.; Emerson, L., Jr. *Chem. Rev.* **1953**, *52*, 121-132. (g) Franck, E. U. In *Proceedings of the 4th International Conference on High Pressure, Kyoto, 1974*; Osugi, J., Ed.; Physico-Chemical Society of Japan: Kyoto, 1975; pp 26-34. (h) Franck, E. U. In *Organic Liquids: Structure, Dynamics and Chemical Properties*; Buckingham, A. D., Lippert, E., Bratos, S., Eds.; Wiley: Chichester, 1978; pp 181-194.

(7) (a) Teherani, T. H.; Bard, A. J. *Acta Chem. Scand., Ser. B* **1983**, *37*, 413-422. (b) Smith, W. H.; Bard, A. J. *J. Am. Chem. Soc.* **1975**, *97*, 5203-5210. (c) Demortier, A.; Bard, A. J. *J. Am. Chem. Soc.* **1973**, *95*, 3495-3500. (d) Uribe, F.; Sharp, P. R.; Bard, A. J. *J. Electroanal. Chem.* **1983**, *152*, 173-182. (e) Teherani, T. H.; Peer, W. J.; Lagowski, J. J.; Bard, A. J. *J. Am. Chem. Soc.* **1978**, *100*, 7768-7770. (f) Werner, M.; Schindewolf, U. *Ber. Bunsenges. Phys. Chem.* **1980**, *84*, 547-550. (g) Saveant, J. M.; Thiebault, A. J. *Electroanal. Chem.* **1978**, *89*, 335-346. (h) Herlem, M.; Minet, J. J.; Thiebault, A. J. *Electroanal. Chem.* **1971**, *30*, 203-217. (i) Laitinen, H. A.; Shoemaker, C. E. *J. Am. Chem. Soc.* **1950**, *72*, 663-665.

(1) (a) McDonald, A. C.; Fan, F. F.; Bard, A. J. *J. Phys. Chem.* **1986**, *90*, 196-202. (b) Flarsheim, W. M.; Tsou, Y.; Trachtenberg, I.; Johnston, K. P.; Bard, A. J. *J. Phys. Chem.* **1986**, *90*, 196-202. (c) Flarsheim, W. M.; Tsou, Y.; Trachtenberg, I.; Johnston, K. P.; Bard, A. J. *J. Phys. Chem.*, in press.

(2) Crooks, R. M.; Fan, F. F.; Bard, A. J. *J. Am. Chem. Soc.* **1984**, *106*, 6851-6852.

(3) (a) Franck, E. U. In *High Pressure Chemistry*; Kelm, H., Ed.; D. Reidel: Boston, MA, 1978; p 243. (b) Nicholls, D. *Inorganic Chemistry in Liquid Ammonia*; Elsevier: Boston, MA, 1979; pp 9-10. (c) Buback, M.; Harder, W. D. *Ber. Bunsenges. Phys. Chem.* **1977**, *81*, 603-614.

(4) Varagafik, N. B., Ed. *Handbook of Physical Properties of Liquids and Gases*, 2nd ed.; Hemisphere: Washington, DC, 1975; pp 464-476.

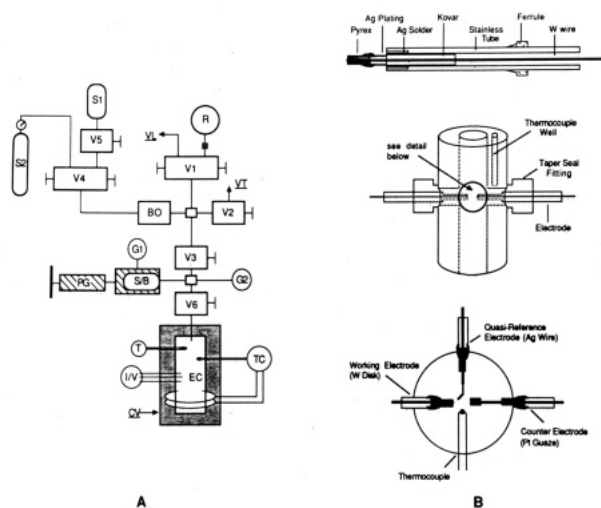


**Figure 1.** (A) Schematic diagram of high-pressure/high-temperature apparatus: V1–V6, high-pressure valves; S1, sample solution; S2, solvent; R, rinse solution; VL, vacuum line connection; BO, blowout disk; VT, vent; G1–2, pressure gauges; PG, pressure generator; S/B, separator with bellows; T, temperature indicator; I/V, electrochemical measurement system; CV, insulated containment vessel; EC, electrochemical cell; TC, temperature controller. (B) (top) Electrode construction details. (middle) Electrochemical cell. (bottom) Detailed view of internal electrode configuration.

SCF. In addition, variation of the dielectric constant and density of supercritical ammonia may allow control over the position of equilibrium in electrosyntheses and simultaneously permit clean separation of product from solvent.

### Experimental Section

**High-Pressure Apparatus.** Construction details of the high-pressure apparatus, electrochemical cell, and electrodes are shown in Figure 1. All home-built sections of the apparatus followed traditional construction techniques for high-pressure and high-temperature applications.<sup>8</sup> The cell was of 314 stainless steel and had a volume of about 7 mL; the total volume of the apparatus during experiments was ca. 20 mL. Stainless steel is resistant to corrosion by ammonia and all other chemicals used in the temperature domain of these experiments; however, the oxides that readily form on the surface of austenitic stainless steels are soluble in ammonia, especially above 100 °C. These surface-passivating oxides, which are crucial to the integrity of stainless steel in aqueous environments, were minimized by allowing the cell to contact a powerful reducing agent (dithionite anion in water) prior to each experiment. Nonetheless, small currents due to the anodic stripping of these metals were occasionally observed in cyclic voltammograms. Recently, a new cell has been fabricated of Inconel 600, a high nickel alloy which is impervious to surface oxidation. The cell was machined from a cylinder 2.5 in. in diameter and 3 in. in length. A  $\frac{3}{8}$ -in. bore was drilled along the longitudinal axis and tapped at either end to accept commercial high-pressure fittings. Similar threads were tapped perpendicular to the central bore midway from the ends to accommodate the electrode feedthroughs. Electrodes were held in place with taper seal high-pressure fittings (High Pressure Equipment, Co., Erie, PA); the distance between working and reference electrodes was always less than 0.3 cm. The experiments described here were performed with an electrode geometry like that shown in Figure 1B. This configuration could lead to contamination of the working solution by species generated at the counter electrode. More recently, we have improved this design by using platinum and

tungsten ultramicroelectrodes (diameter 10–100  $\mu\text{m}$ ), which reduce the current and thus electrogenerated contaminants. Details of this improved apparatus and results obtained by using it will be described in forthcoming papers. The use of unlined metallic cells for electrochemistry can also lead to difficulties in potential control. The problems stem from stray currents that arise in a grounded system; therefore, care was taken to prevent contact of the high-pressure system with earth ground.

The electrodes were constructed by passing a uranium glass-coated tungsten wire (0.040-in. diameter) through a commercially available Kovar to Pyrex seal (Ace Glass, Louisville, KY) and heating to collapse the Pyrex onto the glass-coated wire. The insulating high-pressure seal is formed by the Pyrex/uranium glass seal. This assembly was soldered into a stainless steel tube. The exposed Kovar, which corrodes in ammonia, was electrochemically plated with silver. We have tested the design and found that the electrodes usually fail near 375 bar at 180 °C or 100 bar at 400 °C. Tungsten has proven superior to traditional electrode materials for electrochemistry in ammonia, because it does not catalyze background reactions. For example, the reduction of protons to hydrogen has a 0.5-V overpotential on tungsten as compared to platinum.

The valves, tubing, pressure generator, and fittings were either of 316 or 304 stainless steel (High Pressure Equipment Co., Erie, PA). The pressures reported were measured by a strain gauge pressure transducer (Omega Engineering, Inc., Stamford, CT) in conjunction with a digital voltmeter (Doric, San Diego, CA). The temperature was measured by a stainless steel sheathed internal thermocouple placed within 0.5 cm of the working electrode. Reported temperatures are within  $\pm 2$  °C, and pressures are within  $\pm 4$  bar. All heated regions of the apparatus were safety-shielded by  $\frac{1}{4}$ -in. steel. The low-temperature data were collected by using apparatus similar to that previously described.<sup>7b</sup>

**Chemicals.** Electronics grade nitrobenzene (Kodak, Rochester, NY) was used as received. Quinoxaline (Lancaster Synthesis, Windham, NH), phenazine, and pyrazine (Aldrich Chemical, Milwaukee, WI) were vacuum-sublimed from molecular sieves two or three times and stored in an inert atmosphere. Ammonia (Matheson, anhydrous grade) was distilled twice from sodium prior to use to remove traces of  $\text{O}_2$  and  $\text{H}_2\text{O}$ . In all high-temperature experiments the potassium salt of trifluorosulfonic acid ( $\text{CF}_3\text{SO}_3\text{H}$ ) was used as indifferent electrolyte. The acid (3M Corp., Minneapolis, MN) was neutralized with potassium carbonate and recrystallized three times from acetone. The resulting crystals were dried under vacuum for 2 days at 130 °C, rinsed in liquid ammonia, and dried again under vacuum for 12 h at 130 °C before storing in an inert atmosphere box. Potassium trifluorosulfonate was found to be superior to other electrolytes, since it provided relatively low solution resistance (low ion pairing) in the SCF and is electroinactive within the potential limits of ammonia.

**Procedure.** The working solution was prepared by adding the electrolyte (0.20 M  $\text{CF}_3\text{SO}_3\text{K}$  at 25 °C, falling to 0.14 M in the SCF because of the decrease in density of ammonia) to a 75-mL stainless steel sample vial in an inert atmosphere box. The vial was attached to the vacuum line, and ammonia of a measured volume was distilled into it. The tungsten disk working electrode (area 0.0083  $\text{cm}^2$ ) was polished with 1- $\mu\text{m}$  diamond paste (Buehler, Evanston, IL), rinsed in ethanol, and wiped dry; the silver quasi-reference electrode (Ag QRE) was polished with sandpaper, rinsed, and dried; the platinum gauze counter electrode was briefly soaked in  $\text{HNO}_3$ , rinsed, and dried. The entire apparatus and cell were flushed with ammonia from a solvent reservoir (S2) and then dried under vacuum overnight. The sample vial (S1) was attached to the high-pressure line, and the solution was forced into the cell by gentle heating.

The temperature of the cell was controlled by a digital temperature controller (Omega Engineering, Stamford, CT) attached to a heating tape wrapped around the exterior of the cell. The pressure was adjusted either by venting small amounts of solution as the temperature rose or by adjusting the pressure generator (PG). The concentration of electroactive species was calculated

(8) (a) Bridgman, P. *The Physics of High Pressure*; G. Bell and Sons: London, 1949. (b) Hamann, S. D. *Physico-Chemical Effects of Pressure*; Academic: New York, 1957; pp 7–30. (c) Rössling, G. L.; Franck, E. U. *Ber. Bunsenges. Phys. Chem.* **1983**, *87*, 882–890. (d) Bett, K. E.; Newitt, D. M. In *Chemical Engineering Practice*; Cremer, H. W., Davies, T., Eds.; Butterworths: London, 1958; Vol. 5, pp 196–298. (e) Downs, J. L.; Payne, R. T. *Rev. Sci. Instrum.* **1969**, *40*, 1278–1280.

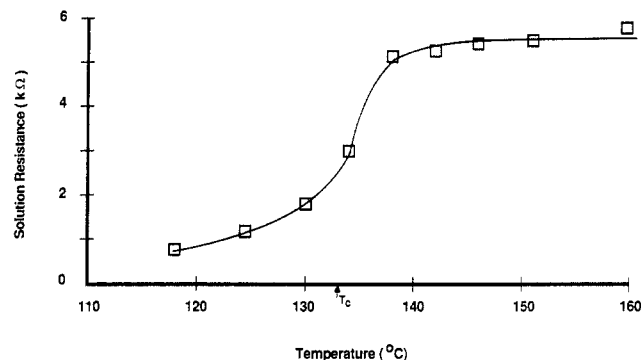


**Figure 2.** Plot of cell resistance ( $R$ ) vs. temperature ( $T$ ) in near-critical and supercritical ammonia. Resistance measurements made by recording the feedback voltage required to minimize the cell time constant for 40-mV, 1-kHz square wave applied to the working electrode. The distance between electrodes was around 0.5 cm. The data were for a constant mass of ammonia. Average electrolyte concentration: 0.15 M  $\text{CF}_3\text{SO}_3\text{K}$ .

from the initial concentration at  $-78^\circ\text{C}$  and the density of ammonia at higher temperatures.<sup>3</sup>

Electrochemical measurements were made by cyclic voltammetry and chronoamperometry.<sup>9</sup> A scan rate of at least 1 V/s was required for cyclic voltammetry to avoid convection, which was manifested as a plateau in the mass-transfer-limited region of the voltammogram. A forward step of 100-ms duration, to a potential at least 100 mV past the peak potentials found by cyclic voltammetry, was used for chronoamperometric measurements. Positive feedback  $iR$  compensation was required to avoid potential control errors. For a typical peak current of 100  $\mu\text{A}$ , the compensated potential amounted to 10 mV at 25  $^\circ\text{C}$  or 40 mV at 150  $^\circ\text{C}$ . Figure 2 shows a plot of relative resistance, measured between the working and reference electrodes, vs. temperature. The resistance measurements were done with a constant mass of ammonia. The increase in resistance reflects the rapid increase of the solution volume and resultant decrease in  $\rho$  near  $T_c$ . The sharply rising portion of the curve centered near  $T_c$  is caused by the reduction in  $\epsilon$  of the solvent as it becomes supercritical and demonstrates that  $T_c$  is not substantially changed by the addition of electrolyte. The latter conclusion agrees with that of Silvestri et al.<sup>10</sup> for KI in supercritical ammonia.

**Electrochemical Equipment.** All electrochemical measurements were made using a Princeton Applied Research Model 173 potentiostat/galvanostat and Model 175 universal programmer. Data were collected on a Norland Model 3001 processing digital oscilloscope.

**Reference Potentials.** Thermodynamically meaningful reference electrodes are difficult to construct for use at elevated temperature and pressure. There have been two strategies for dealing with the high-temperature regime:<sup>11</sup> placement of a standard reference electrode directly within the high-temperature solution or isolation of the reference electrode in a room-temperature environment with a salt bridge contact to the working solution. There are difficulties with both of these approaches. In the case of the internal standard hydrogen electrode, a pressure of hydrogen must be maintained over a platinum substrate in such a way as to avoid contamination of the working solution. In water this has been accomplished up to 275  $^\circ\text{C}$  for the calibration of secondary electrodes,<sup>11,12</sup> but because of the unique characteristics of the supercritical phase, a suitable primary or secondary internal reference has, to our knowledge, not been devised. In the case of an external reference electrode one must accept unknown thermal, bridge, and liquid

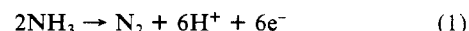
junction potential gradients, as well as large potential control errors in solutions with high resistance. Little quantitatively consistent success has been achieved in solutions with large temperature differentials.

The Ag QRE has many qualities which make it an excellent standard electrode for SCF: it is simple to build, is rugged, and provides a stable reference potential for a sufficient length of time.<sup>13</sup> In addition, it does not require an associated ion in solution. Such ions, especially halides, could be oxidized at the counter electrode of the one-compartment cell and subsequently interfere with reactions at the working electrode. Furthermore, most salts are of limited solubility in supercritical ammonia or they ion pair extensively and are of unknown and highly variable activity. For these reasons and for lack of a suitable alternative, the Ag QRE was the reference electrode of choice for potential measurements in ammonia and other SCF systems. As long as the potential of the QRE does not change during the measurement, its potential can be determined with respect to a more thermodynamically meaningful potential by the use of a reference redox couple. For example, in many nonaqueous solvents the ferrocene/ferrocenium couple is employed. In ammonia it is convenient to use the onset of solvated electron generation ( $e_s^-$ ) as a reference. In our solution the potential for the Ag QRE did not change ( $\pm 20$  mV) in pure electrolyte vs. the onset of  $e_s^-$  from 25 to 150  $^\circ\text{C}$ , and thus we report all potentials vs.  $e_s^-$ . In pure electrolyte solutions a current density due to  $e_s^-$  of 24.1  $\text{mA}/\text{cm}^2$  occurred at  $-1.68 \pm 0.02$  V vs. Ag QRE between 25 and 150  $^\circ\text{C}$  (scan rate 1 V/s). The electrochemical solvation of electrons in liquid ammonia is known to be a reversible process,<sup>27a</sup> and Laitinen and Nyman<sup>14</sup> found the "electron electrode" to be quite reliable. In addition, Schindewolf and Werner<sup>15</sup> found the potential of the electron electrode to be practically independent of temperature between  $-35$  and  $-75^\circ\text{C}$ . The dianion of nitrobenzene precipitated onto the surface of the working electrode, altering the thermodynamic potential for subsequent  $e_s^-$  formation. In that case potentials were obtained directly from the QRE but reported vs.  $e_s^-$ .

## Results and Discussion

**Cyclic Voltammetric Reduction of Aza Aromatics.** Cyclic voltammograms for pure supporting electrolyte at 25 and 150  $^\circ\text{C}$  are shown in Figure 3A. No significant faradaic processes are observed from +2.1 to +0.2 V (vs.  $e_s^-$ ) at 25  $^\circ\text{C}$ . However, in the SCF a small anodic wave near +1.7 V is evident. This feature corresponds to the anodic stripping of trace metal impurities dissolved as oxides from the surface of the stainless steel cell. The results reported were not significantly affected by this process; recent experiments in an Inconel cell do not show the metal stripping peak and give results identical with those reported here.

Initial experiments utilizing alkali metal halides, mainly KI, as supporting electrolytes in the SCF occasionally showed spurious currents, particularly near the positive potential limit in the presence of aromatic species. The limiting potential in these cases, +2.0 V at 150  $^\circ\text{C}$ , was attributed to the oxidation of halide<sup>16</sup> that either was reactive toward the electroactive species or could itself be reduced at the working electrode. No such interferences were observed in the presence of  $\text{CF}_3\text{SO}_3\text{K}$ , because the anodic background process, which begins +2.4 V at 150  $^\circ\text{C}$ , is probably oxidation of  $\text{NH}_3$ :



Care was taken to keep cell currents small so as to minimize contamination of the solution by  $\text{H}^+$ , since it reacts with most of the species studied. The available potential window for electrochemistry in ammonia at  $-70^\circ\text{C}$  is around 3.0 V. This range decreases to 2.6 V at 25  $^\circ\text{C}$  and 2.2 V 150  $^\circ\text{C}$ , presumably because

(9) Bard, A. J.; Faulkner, L. R. *Electrochemical Methods*; Wiley: New York, 1980; pp 142–145, 213–235.

(10) Silvestri, G.; Gambino, S.; Gilardo, G.; Cuccia', C.; Guarino', E. *Angew. Chem., Int. Ed. Engl.* **1981**, *20*, 101–102.

(11) Jones, D. de G.; Masterson, H. G. In *Advances in Corrosion Science and Technology*; Fontana, M. G., Staehle, R. W., Eds.; Plenum: New York, 1970; Vol. 1, pp 1–49 and references therein.

(12) MacDonald, D. D. *Corrosion* **1978**, *34*, 75–84 and references therein.

(13) Hills, G. J. *Reference Electrodes: Theory and Practice*; Ives, D. J. G., Janz, G. J., Eds.; Academic: New York, 1961; pp 433–460.

(14) Laitinen, H. A.; Nyman, C. J. *J. Am. Chem. Soc.* **1948**, *70*, 3002–3008.

(15) Schindewolf, U.; Werner, M. *J. Phys. Chem.* **1980**, *84*, 1123–1127.

(16) Schmidt, V. H.; Meinert, H. *Z. Anorg. Allg. Chem.* **1958**, *295*, 156.

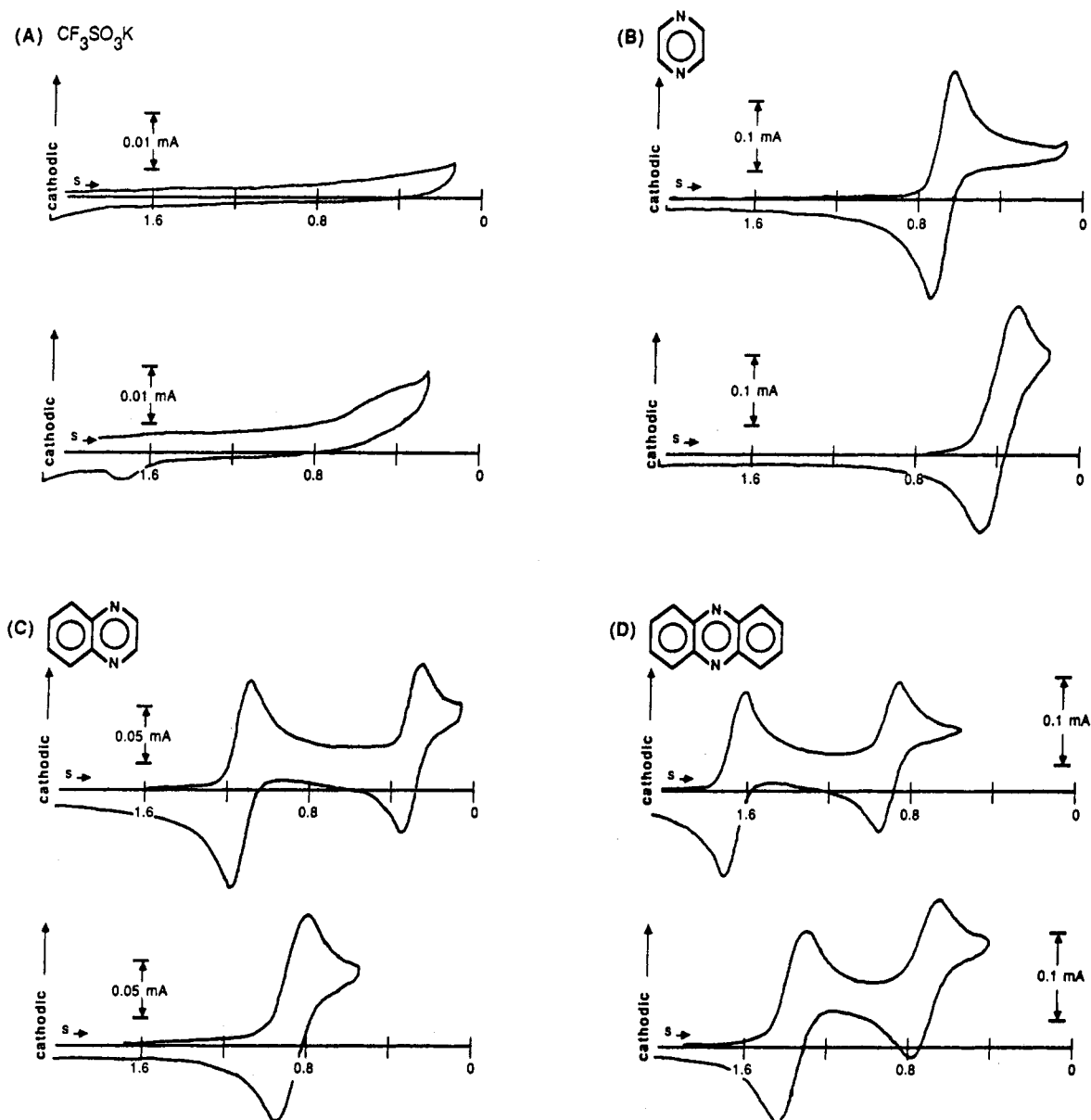


**Figure 3.** Cyclic voltammetry in ammonia/CF<sub>3</sub>SO<sub>3</sub>K at a W working electrode (0.0083 cm<sup>2</sup>). (A) Supporting electrolyte only: top, 0.20 M; bottom, 0.14 M. (B) Pyrazine: top, 6.5 mM; bottom, 4.6 mM. (C) Quinoxaline: top, 3.6 mM; bottom, 2.6 mM. (D) Phenazine: top, 4.3 mM; bottom, 3.2 mM. In all cases the top voltammogram was taken at 25 °C and 9.5 bar and the bottom at 150 °C and 285 bar (supercritical). The concentration varies because of differences in solvent density. Scan rate = 2 V/s. Potentials are vs. the onset of e<sub>s</sub><sup>-</sup>.

**TABLE II: Summary of Voltammetric and Chronoamperometric Parameters for Reduction of Organics in Ammonia**

reduction temp, °C	pyrazine		quinoxaline			phenazine				nitrobenzene		
	1	150	1	2	25	1	2	150	1	150	-40	
$i_{pa}/i_{pc}^a$	1.01	0.99	1.01	1.01	1.09	0.99	0.98	1.04	1.12	1.03	0.92	1.0
$i_{pc}^a/v^{1/2}C_s^a$ (A s <sup>1/2</sup> cm <sup>3</sup> )/(V mol)	17.9	28.8	17.9	29.0	15.1	18.3	28.6	16.2	23.4	17.6	37.7	12.9
$E_{p,c}^a$ V vs. e <sub>s</sub> <sup>-</sup>	0.63	0.32	1.10	0.81	0.30	1.55	1.25	0.84	0.62	1.50	1.30	0.36 <sup>b</sup>
$\Delta E_{p,c}^a$ mV	94	150	78	128	74	76	116	78	116	114	160	63
diffusion coeff × 10 <sup>4</sup> , cm <sup>2</sup> /s	1.0	5.1	0.77	3.2	c	0.75	3.0	c	c	0.99	4.3	0.27
act. energy for diffusion × 10 <sup>-4</sup> , J/(mol K)	1.3		1.2		c	1.1		c			1.2	
$dE_{1/2}/dT$ , mV/°C	-2.5		-2.3		-2.5	-2.5		-2.2			-1.9	
$\Delta S_{rxn}^c$ × 10 <sup>-2</sup> , J/(mol K)	-2.4		-2.2		-2.4	-2.4		-2.1			-1.8	

<sup>a</sup>See ref 9. <sup>b</sup>Potentials vs. Ag QRE. <sup>c</sup>Data unavailable.

of more facile kinetics of the anodic background process, eq 1, at the higher temperatures.

The general electrochemical reaction scheme expected in aprotic media for the aza aromatics is<sup>17</sup>



However, a variety of reactions of R<sup>•-</sup> and R<sup>2-</sup> that follow electron-transfer reactions are known to occur (e.g., disproportionation, dimerization, and synproportionation). In the presence of a proton

(17) Baumgartel, H.; Retzlav In *Encyclopedia of Electrochemistry of the Elements*; Bard, A. J., Lund, H., Eds.; Marcel Dekker: New York, 1984; pp 168-317.

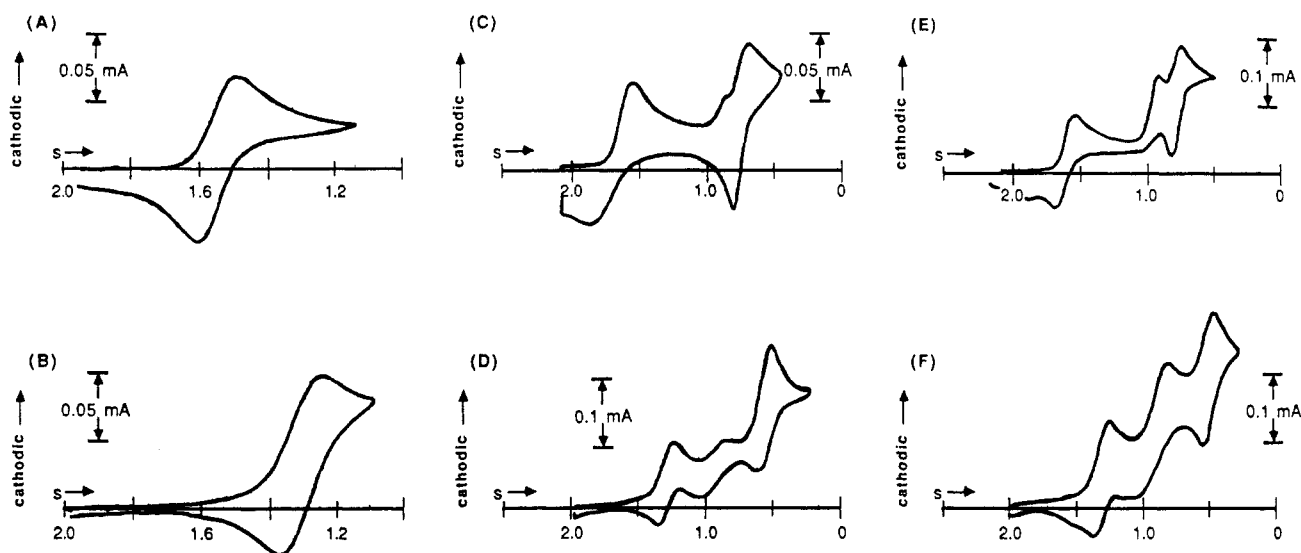


**Figure 4.** Cyclic voltammetry of nitrobenzene (NB) in ammonia/ $\text{CF}_3\text{SO}_3\text{K}$ . First reduction only: (A) 25 °C, 9.5 bar,  $C_{\text{NB}} = 4.1$  mM; (B) 150 °C, 285 bar (supercritical),  $C_{\text{NB}} = 2.7$  mM. First and second reduction in the presence of a trace of water: (C) 25 °C, 9.5 bar,  $C_{\text{NB}} = 4.1$  mM; (D) 150 °C, 285 bar (supercritical),  $C_{\text{NB}} = 2.7$  mM. Reduction in the presence of approximately 1:1 water/NB: (E) 25 °C, 9.5 bar,  $C_{\text{NB}} = 5.33$  mM; (F) 150 °C, 285 bar (supercritical),  $C_{\text{NB}} = 3.51$  mM. Scan rate = 1 V/s. Potentials vs.  $e_s^-$ .

source, particularly at elevated temperature, follow-up chemistry can occur which might complicate the simple stepwise electron-transfer mechanisms shown in eq 2 and 3.

Typical voltammograms of the nitrogen heterocycles pyrazine (PYR), quinoxaline (QUIN), and phenazine (PHEN) at 25 and 150 °C are shown in Figure 3B–D. The data derived from these voltammograms are summarized in Table II. For a stable reaction product produced by a reversible electron transfer the ratio of the peak anodic and cathodic currents ( $i_{p,a}/i_{p,c}$ ) is equal to one. A ratio near unity was found experimentally for all of the aza aromatics. In cyclic voltammetry the cathodic current function,  $i_{p,c}/v^{1/2}C$ , where  $v$  is scan rate and  $C$  the bulk concentration, is constant for diffusion-controlled systems at different values of  $v$ . Experimentally, the standard deviations of the current functions never exceeded 5% at 25 °C or 10% at 150 °C for scan rates of 1–20 V/s. The values for  $\Delta E_p$  ranged from 76 to 94 mV at 25 °C and from 116 to 150 mV at 150 °C (compared to theoretical Nernstian one-electron values of 59 and 84 mV, respectively).<sup>18</sup> The potential of the peak cathodic current,  $E_{p,c}$ , shifted slightly in a negative direction with scan rate, especially in the SCF.

The current-based diagnostics indicate the product of the electrochemical process occurring at the potential of the first wave for QUIN and PHEN is stable. The potential-dependent measurements suggest a reversible electron transfer, but at fast scan rates they vary somewhat from ideality, particularly in the SCF. These deviations from the theoretical values of the potential diagnostics are due to uncompensated solution resistance, especially at rapid scan rates, rather than real deviations of the electrode reactions from Nernstian behavior. Recent experiments with ultramicroelectrodes (area ca.  $10^{-5}$  cm<sup>2</sup>) have shown that  $\Delta E_p$  for the first reduction of PHEN is constant at  $v$  up to 50 V/s. Based on the evidence presented in Table II and supporting evidence from chronoamperometric data to be discussed later, the first waves of PHEN and QUIN, in liquid and supercritical ammonia, are assigned to one-electron reversible processes, as shown in eq 2. The value of  $\Delta E_p$  is significantly larger for PYR than for either QUIN or PHEN. This might represent a limitation of the heterogeneous electron-transfer rate; therefore, the reduction of PYR is quasi-reversible.

No second reduction was noted for PYR even in experiments performed at –40 °C. A second voltammetric wave was observed at 25 °C for QUIN, but it faded into the cathodic background process at 100 °C. At both room temperature and in the SCF two waves were present for the reduction of PHEN. The ex-

perimental parameters derived from cyclic voltammetry for the second reductions of QUIN and PHEN at 25 and 150 °C are shown in Table II.

At 25 °C the voltammetric diagnostics for the second wave of QUIN are consistent with that of the first, and by similar arguments, it is assigned as a reversible, one-electron transfer. The slightly high value of  $i_{p,a}/i_{p,c}$  usually is suggestive of a surface process, such as adsorption or precipitation, but is attributed here to the difficulty of measuring the peak current of a second cyclic voltammetric wave.<sup>19</sup> In those cases where a second wave is present in the voltammetry, the current function for the second wave is slightly smaller than that of the first. Theoretically, if both waves represent reversible electron transfer, the current function should be the same. The aforementioned difficulty of measuring  $i_{p,c}$  for the second wave accounts for this inconsistency.

The utility of ammonia as an aprotic solvent is especially evident in the case of PHEN, which shows a well-developed second wave even in the SCF. At 25 °C this wave is reversible, and even at 150 °C, the current function,  $i_{p,a}/i_{p,c}$ , and  $\Delta E_p$  point to Nernstian behavior. Previous work has demonstrated the unique stability of the radical anions and dianions of nitrobenzene and benzophenone in liquid ammonia at –40 °C.<sup>7a-c</sup> It has been suggested that this stability was mainly due to the low temperature of the solvent, but slow sweep voltammetry in the SCF at 150 °C shows the dianion of PHEN ( $\text{PHEN}^{2-}$ ) to have a half-life ( $t_{1/2}$ ) in excess of 0.5 min, and initial coulometric measurements of the anion radical ( $\text{PHEN}^{\cdot-}$ ) indicate  $t_{1/2} > 3$  min. On the basis of these results we conclude the stability of  $\text{PHEN}^{\cdot-}$  and  $\text{PHEN}^{2-}$  is due to the intrinsic nature (i.e., low acidity) of ammonia rather than only to temperature effects.

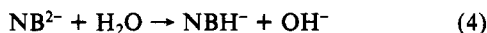
**Cyclic Voltammetric Reduction of Nitrobenzene.** The electrochemistry of nitrobenzene (NB) in ammonia at –40 °C has been elucidated in the absence and presence of weak and strong acids.<sup>7b</sup> In the absence of an acid, two reversible one-electron transfers corresponding to eq 2 and 3 were found where  $E_{p,c,1} = -0.44$  V and  $E_{p,c,2} = -1.26$  V vs. Ag/AgI QRE. With an available proton in solution, the voltammetry became more complicated and is discussed below. We have investigated those systems at elevated temperature and pressure in order to compare their behavior over a temperature range of nearly 200 °C. Such information should be useful for extrapolating other low-temperature data into the supercritical regime.

(19) Techniques generally used to discern information from the voltammetry of multistep charge transfers were ineffective on account of convection (ref 9, pp 232–236.); therefore, the semiempirical method suggested by Nicholson was applied (Nicholson, R. S. *Anal. Chem.* **1966**, *38*, 1406).

Figure 4, A and B, shows the voltammetry of the first reduction of NB at 25 and 150 °C, respectively. The diagnostic parameters derived from these voltammograms are collected in Table II. The behavior of the first reduction of NB is quite similar to that of the first reduction at low temperature, except for the values of  $\Delta E_p$ . At 25 and 150 °C  $\Delta E_p$  was found to be nearly twice as high as the theoretical value for a reversible electron transfer; however, even at -40 °C there was a 10% departure from the Nernstian value. Since  $\Delta E_p$  is significantly larger for the first reduction of NB than for that of either PHEN or QUIN at  $v = 2$  V/s and since the solution resistance should be the same in both cases, it must represent a real deviation of the associated electron-transfer reaction from reversibility. On the basis of work at -40 °C and chronoamperometric data and by analogy to arguments made for PYR, this reduction is assigned as a quasi-reversible one-electron transfer.

Figure 4C shows the more complex voltammetric response of NB at 25 °C when the potential is scanned past the first reduction. By analogy to the cyclic voltammetric behavior of NB at -40 °C (ref 7b, Figure 3), two one-electron waves are expected for this system; however, additional features are present. Particularly prominent are a small cathodic prewave at +0.88 V and a shoulder on the first anodic wave centered at +1.91 V. The voltammogram shown in Figure 4C can be explained by an inextirpable trace of water present in the high-pressure apparatus which acts as a weak acid as was shown for the reduction of NB in liquid ammonia at -40 °C (ref 7b, Figure 5). When water was intentionally added to the NB system at 25 °C, the two anomalous waves present in Figure 4C became larger (Figure 4E).

The prewave at +0.88 V (Figure 4C) is indicative of a following chemical reaction, in this case the protonation of the dianion of NB ( $\text{NB}^{2-}$ ) by water.



After this step,  $\text{NBH}^-$  rapidly decomposes to  $\text{OH}^-$  and nitrosobenzene ( $\text{PhNO}$ ). The latter is immediately reduced to  $\text{PhNO}^{2-}$  and takes on a proton to form  $\text{PhNOH}^-$ . Upon scan reversal the two oxidation waves of  $\text{NB}^{2-}$  at +0.75 and +1.66 V dominate the voltammetry, but a slight broadening on the positive side of the anodic wave at +0.75 V is evident, as is the small wave at +1.91 V. These features are due to the oxidation of  $\text{PhNOH}^-$  to  $\text{PhNOH}^{\bullet}$  (which deprotonates quickly to the radical anion) and further oxidation of  $\text{PhNO}^-$  to  $\text{PhNO}$ .

The single difference between the voltammetry presented here and that of the previous study with isopropyl alcohol (IPA) as proton donor is the relative position of the prewave (Figure 4C, at +0.88 V). At -40 °C this prewave was shifted in a negative direction by 0.2 V relative to the following wave. Because water is a stronger acid than IPA in ammonia, such a shift is expected and reflects an increase in the equilibrium constant of eq 4.

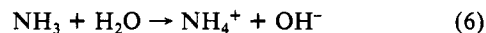
With the exception of the two small waves just discussed, the electrochemistry of NB at 25 °C is found to be in qualitative agreement with the behavior at -40 °C in the absence of acid. Especially significant features present in the voltammetry at both +25 °C and -40 °C are the surfacelike anodic wave at +0.75 V, which corresponds to the oxidation of precipitated  $\text{NB}^{2-}$  and the identical splitting between the two cathodic waves of 0.82 V. Therefore, the cathodic wave present at +0.68 V in the voltammetry of NB at 25 °C must correspond to a quasi-reversible reduction of the radical anion of NB ( $\text{NB}^{\bullet-}$ ) to the insoluble  $\text{NB}^{2-}$  salt.

The voltammetry at 150 °C is substantially different than that at 25 °C. Figure 4D,F shows the voltammetric response at 150 °C, which corresponds to the two NB/ $\text{H}_2\text{O}$  voltammograms of Figure 4C,E at a lower temperature. Figure 4D shows that the prewave has shifted positive by an additional 0.2 V relative to the second reduction wave. The peak current of the second reduction near +0.48 V has more than doubled, relative to the first, and the anodic back-wave associated with precipitation of  $\text{NB}^{2-}$  at 25 °C is greatly reduced. In addition, the anodic wave due to the oxidation of  $\text{PhNO}^{\bullet-}$  at 25 °C is absent. This behavior is quite similar to that found at -40 °C for the reduction of NB in the

presence of a strong acid (ref 7b, Figure 8). In that case the mechanism was found to be analogous to that of the weak acid, except  $\text{PhNOH}^-$  added an additional proton to form neutral phenylhydroxylamine ( $\text{PhNOH}_2$ )



which can only be oxidized at potentials positive of the solvent limit at 150 °C. We cannot give a complete quantitative explanation of the voltammetry of the NB system at 150 °C at this time, but the evidence suggests that water in ammonia acts as a stronger acid toward  $\text{NB}^{2-}$  at 150 °C than at 25 °C. Little information is available on acid-base chemistry in ammonia at elevated temperatures,<sup>20</sup> and there have been no direct measurements of acidity as a function of temperature; however, there is ample indirect evidence that acidity should increase with temperature. First, the acidity of water and aqueous acids increases with temperature: for example, the autoprotolysis constant of water,  $K_w$ , increases by 2 orders of magnitude between 25 and 150 °C.<sup>21</sup> Jolly<sup>22</sup> calculated the equilibrium constant ( $K$ ) for the reaction



in  $\text{NH}_3$  to be about  $2 \times 10^{-20}$  at 25 °C based on thermodynamic estimates. Schindewolf and Schwab<sup>23</sup> measured  $K$  experimentally at -40 °C and found it to be  $6.3 \times 10^{-22}$ . He suggested that the discrepancy in  $K$  was due part to the uncertainty of the thermodynamic estimates but also that the temperature difference of 65 °C probably resulted in an increase of  $K$  by an order of magnitude.

The effect of an increase in the acidity of water is to increase the equilibrium concentration of  $\text{NBH}^-$  (eq 4) and thus the magnitude of the cathodic wave near +0.48 V (Figure 4D). In addition, the positive shift of the cathodic prewave (+0.88 V, Figure 4D) is also consistent with an increase in acidity. Additionally, more of the  $\text{PhNOH}^-$  should protonate to form  $\text{PhNOH}_2$  (eq 5), leading to the observed decrease in the anodic wave at +0.63 V and the absence of a current related to the oxidation of  $\text{PhNO}^{\bullet-}$ . At rapid scan rates ( $v > 20$  V/s), the voltammetry of Figure 4D approached that of Figure 4C. This implies that the kinetics of eq 4 and 5 are sufficiently slow that the rate increase associated with the enhanced acidity of water can be offset by a decrease in the time frame of the experiment.

**Diffusion Coefficients.** The measured diffusion coefficients ( $D$ ) of aromatics at 25 °C and in the SCF are given in Table II. These were obtained for potential steps past  $E_{p,c}$  of the first, one-electron, wave and for the second wave ( $n = 2$ ) for PHEN. The integrated chronoamperometric behavior<sup>9</sup> is shown in Figure 5.

A uniform fourfold change in  $D$  is found between 25 and 150 °C, with about an order of magnitude change between -40 and +150 °C. This change can be compared to that predicted by various models (e.g., the Stokes-Einstein equation and the activated diffusion model) to draw conclusions regarding the structure of near-critical and supercritical ammonia and other fluids. The Stokes-Einstein (S-E) relationship

$$D = kT/6\pi r\eta \quad (7)$$

(where  $k$  is Boltzmann's constant,  $r$  the radius of the diffusing particle, and  $\eta$  the viscosity of the medium) is based on the model of a macroscopic sphere moving in an incompressible, continuous fluid. The molecules chosen for this study do not closely approach being spheres, and the electrolyte is not continuous but composed of ions and molecules roughly the same size as the diffusing

(20) (a) Birchall, T.; Jolly, W. L. *J. Am. Chem. Soc.* **1965**, *87*, 3007-3008. (b) Cuthrell, R. E.; Fohn, E. C.; Lagowski, J. J. *Inorg. Chem.*, **1966**, *5*, 111-114. (c) Takemoto, J. H.; Lagowski, J. J. *Inorg. Nucl. Chem. Lett.* **1970**, *6*, 315-319.

(21) (a) Robertson, R. E.; Scott, J. M. W.; Golding, P. D. *J. Am. Chem. Soc.* **1981**, *103*, 5923-5925. (b) Noyes, A. A.; Kato, Y.; Sosmun, R. B. *Z. Phys. Chem.* **1910**, *73*, 1-24.

(22) Jolly, W. L. *Adv. Chem. Ser.* **1965**, No. 50, 27.

(23) Schindewolf, U.; Schwab, H. *J. Am. Chem. Soc.* **1981**, *85*, 2707-2708.

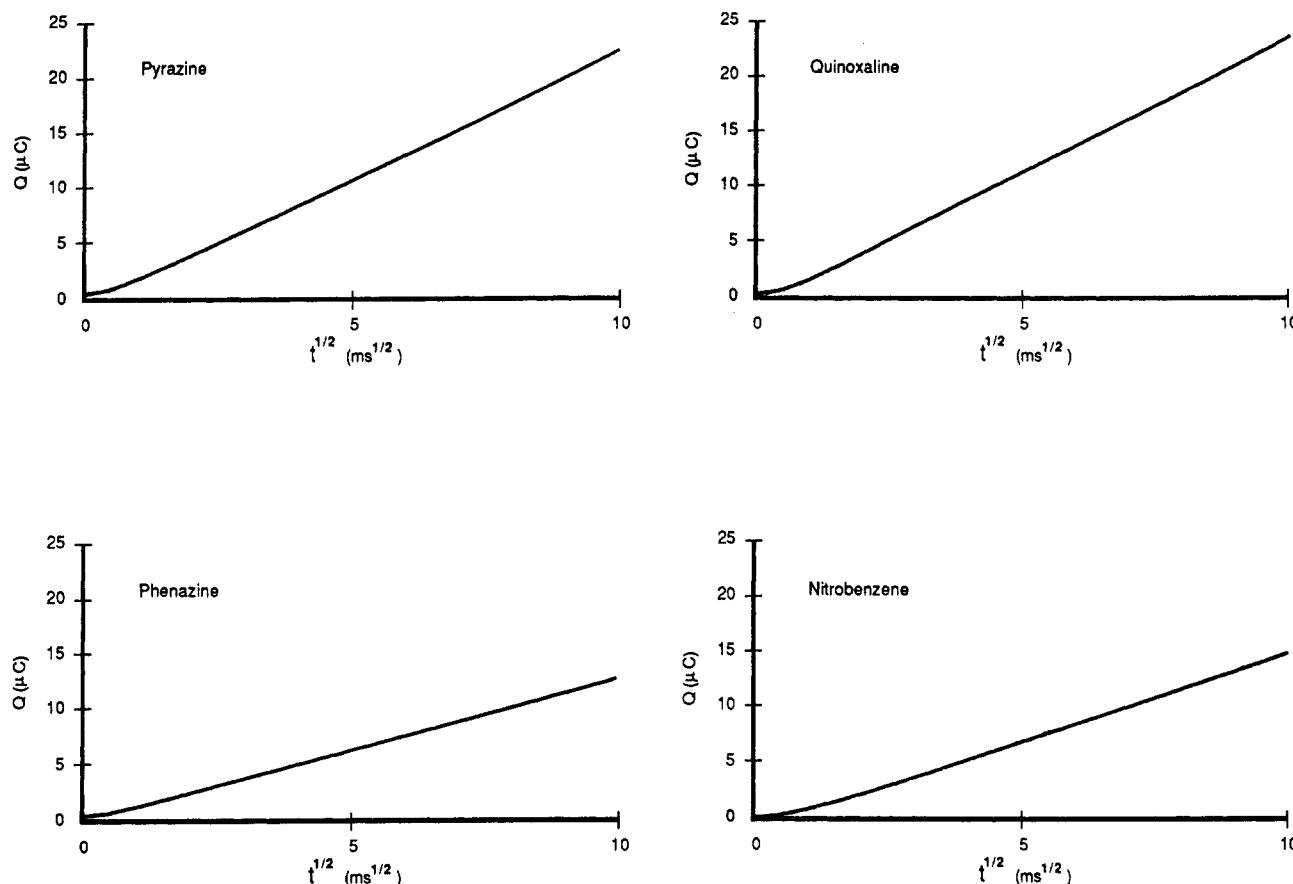


**Figure 5.** Representative plots of charge ( $Q$ ) vs.  $t^{1/2}$  derived from the integrated chronoamperometric response of aromatics in supercritical ammonia at a W electrode ( $0.0083 \text{ cm}^2$ ): (A) 4.59 mM pyrazine, slope =  $2.28 \mu\text{C}/\text{ms}^{1/2}$ ; (B) 6.55 mM quinoxaline, slope =  $2.37 \mu\text{C}/\text{ms}^{1/2}$ ; (C) 3.96 mM phenazine, slope =  $1.27 \mu\text{C}/\text{ms}^{1/2}$ ; (D) 3.88 mM nitrobenzene, slope =  $1.58 \mu\text{C}/\text{ms}^{1/2}$ . Conditions:  $T = 150 \text{ }^\circ\text{C}$ ;  $P = 285 \text{ bar}$ ; electrolyte, 0.14 M  $\text{CF}_3\text{SO}_3\text{K}$ . All concentrations corrected for changes in the density of ammonia. The diffusion coefficients reported in Table II represent the average of several independent experiments.

particles. Nonetheless, S-E has frequently been invoked for such liquids and occasionally for supercritical media.<sup>1,24</sup> The values of  $D$  in Table II are in qualitative agreement with such a model; that is, the larger molecules have smaller diffusion coefficients. Figure 6 shows plots of  $D$  vs.  $T$  from 25 to 150  $^\circ\text{C}$  for the neutral aza aromatics and NB. The points are correlated by a line which represents the S-E relationship based on the experimentally determined value of  $r$  at 25  $^\circ\text{C}$ . The data adhere reasonably well to the theoretical model, except in the case of PYR, where a positive deviation is observed. This deviation may be caused by the close proximity of the PYR wave to the cathodic background process at elevated temperature and probably does not represent a real deviation from S-E behavior. The overall agreement between theory and experiment suggests that the hydrodynamic assumptions inherent in S-E apply to near-critical and supercritical ammonia. Moreover, the basic fluid structure of ammonia and the solvation sphere of the particles do not change radically with increasing temperature. Similar results were found in previous studies in supercritical water.<sup>1,24</sup>

The energy of activation for diffusion ( $E_A$ ) can be obtained from a plot of  $\ln D$  vs.  $1/T$  (Figure 7) according to the equation

$$D = D^* \exp[-(E_A/RT)] \quad (8)$$

A deviation from linearity of these plots would imply a marked structural change of the solvated species.<sup>25</sup> No evidence of such behavior is present in Figure 7; this supports the earlier conclusion that the nature of diffusion and solvation in the SCF is similar to that of room-temperature solutions. Table II lists numerical values for  $E_A$  derived from Figure 7. These values are in accord

with those found in previous investigations for diffusion in aqueous media.<sup>1,26</sup>

**Solvated Electrons.** Solvated electrons ( $e_s^-$ ) have been prepared in a variety of solvents such as liquid ammonia, dimethyl sulfoxide, water, and propylene carbonate.<sup>27</sup> Electrons may exist in quasi-free and localized states, as well as in the stabilized solvated state,<sup>27h</sup> but in which of these modes they are found in a particular setting has been the subject of much discussion. Recently, electrons have been injected into supercritical water and ammonia by photolysis and pulse radiolysis.<sup>28</sup> These investigations have been primarily aimed at the determination of the state of the electrons as a function of solvent density and time, but Krebs<sup>29</sup> has suggested that information from such experiments could also serve as a useful probe of the structure of supercritical ammonia.

(26) Mallouk, T. E.; Cammarata, V.; Crayston, J. A.; Wrighton, M. S. *J. Phys. Chem.*, in press.

(27) For previous studies of  $e_s^-$  in ammonia, see: (a) Teherani, T.; Itaya, K.; Bard, A. J. *Nouv. J. Chim.* **1978**, *2*, 481-487. (b) Schindewolf, U. *Angew. Chem., Int. Ed. Engl.* **1968**, *7*, 190-202. (c) Bard, A. J.; Itaya, K.; Malpas, R. E.; Teherani, T. *J. Phys. Chem.* **1980**, *84*, 1262-1266. (d) Uribe, F. A.; Sawada, T.; Bard, A. J. *Chem. Phys. Lett.* **1983**, *97*, 243-246. (e) Jolly, W. L. In *Metal-Ammonia Solutions*; Lagowski, J. J., Sienko, M. J., Eds.; Butterworths: London, 1970; pp 168-181. (f) Lepourte, G.; Jortner, J. *J. Phys. Chem.* **1972**, *76*, 683-687. (g) Postl, D.; Schindewolf, U. *Ber. Bunsenges. Phys. Chem.* **1971**, *75*, 662-665. (h) Krohn, C. E.; Antoniewicz, J. C.; Thompson, J. C. *Surf. Sci.* **1980**, *101*, 241.

(28) (a) Jortner, J.; Gaathon, A. *Can. J. Chem.* **1977**, *55*, 1801-1819. (b) Krebs, P.; Wanschik, M. *J. Phys. Chem.* **1980**, *84*, 1155-1160. (c) Thompson, J. C.; Even, U.; Blanks, D. K. *J. Phys. Chem.* **1984**, *88*, 3709-3711. (d) Krebs, P.; Bukowski, K.; Giraud, V.; Heintze, M. *Ber. Bunsenges. Phys. Chem.* **1982**, *86*, 879-887. (e) Olinger, R.; Hahne, S.; Schindewolf, U. *Ber. Bunsenges. Phys. Chem.* **1972**, *76*, 349-350. (f) Giraud, V.; Krebs, P. *Chem. Phys. Lett.* **1982**, *86*, 85-90. (g) Krebs, P. *J. Phys. Chem.* **1984**, *88*, 3702-3709. (h) Krebs, P.; Heintze, M. *J. Chem. Phys.* **1982**, *76*, 5484-5492.

(29) Krebs, P. *Chem. Phys. Lett.* **1980**, *70*, 465-468.

(24) Lamb, W. J.; Hoffman, G. A.; Jonas, J. *J. Chem. Phys.* **1981**, *74*, 6875-6880.

(25) Bockris, J. O'M.; Reddy, A. K. N. *Modern Electrochemistry*; Plenum: New York, 1977; pp 544-547.

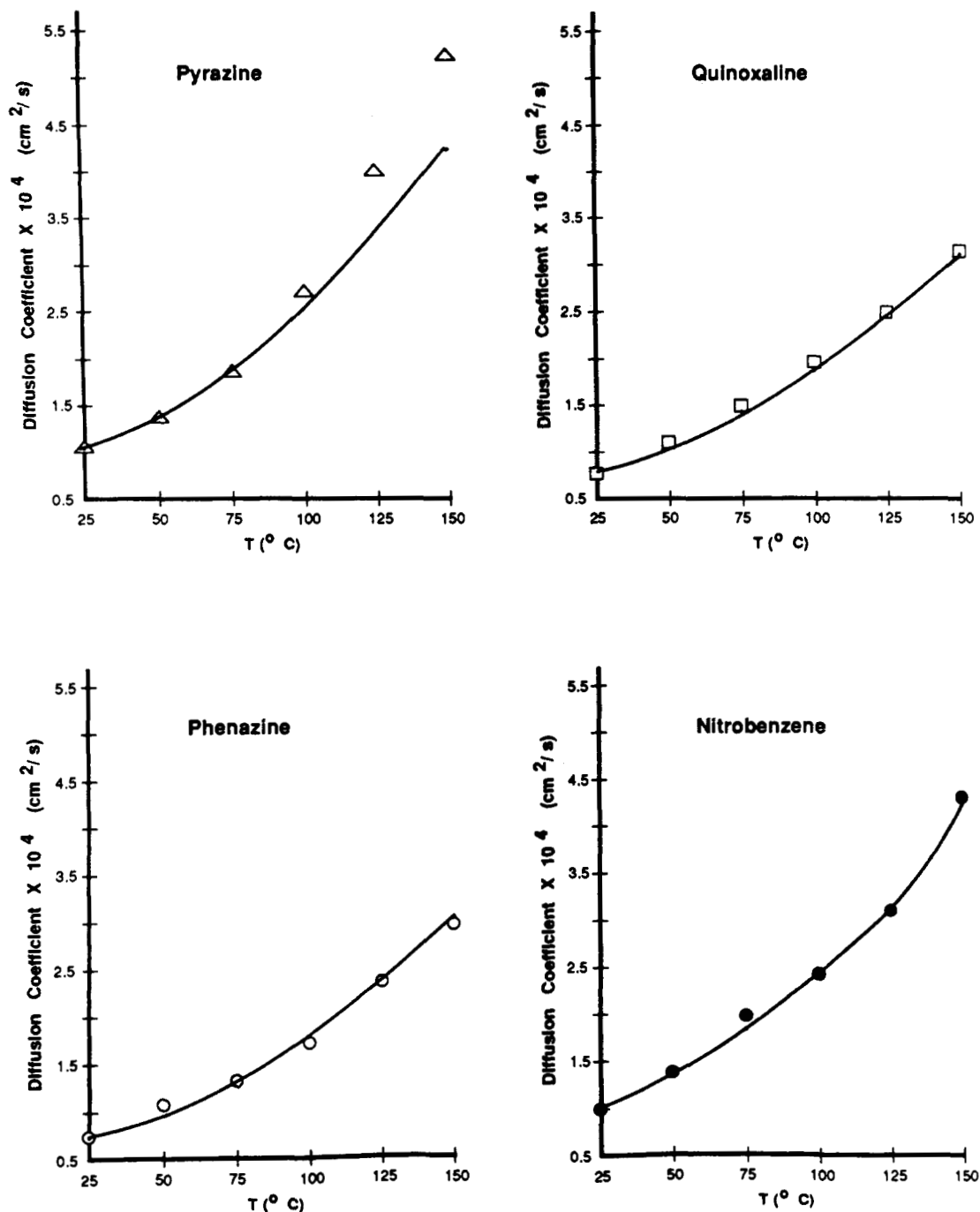
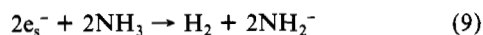


Figure 6. Dependence of the diffusion coefficient on temperature. The points represent experimental data, and the solid line represents the Stokes-Einstein fit based on the experimentally determined effective molecular radius at 25 °C: (A) pyrazine,  $r = 1.45 \text{ \AA}$ ; (B) quinoxaline,  $r = 1.89 \text{ \AA}$ ; (C) phenazine,  $r = 1.94 \text{ \AA}$ ; (D) nitrobenzene,  $r = 1.45 \text{ \AA}$ .

In an earlier report on electrochemistry in supercritical ammonia,<sup>2</sup> we showed the first evidence of electrogeneration of  $e_s^-$  in a SCF but were unable to observe a current from reoxidation at scan rates up to 100 V/s. We interpreted this result as a fast reaction between  $e_s^-$  and  $\text{NH}_3$



and concluded that the  $e_s^-$  half-life ( $t_{1/2}$ ) was too short to be measured by voltammetric techniques at usual scan rates. In scrupulously clean metal-ammonia solutions and in the absence of any catalyst, eq 9 is quite slow; at  $-70 \text{ }^\circ\text{C}$ ,  $t_{1/2}$  ca. 1 year, and at  $25 \text{ }^\circ\text{C}$ ,  $t_{1/2}$  ca. 300 h.<sup>27e</sup> The concentration of an electrochemically generated solution of  $e_s^-$  in 0.1 M KI decreased by only 3–7% in 3 h at  $-55 \text{ }^\circ\text{C}$ ;<sup>27a</sup> however, eq 9 could become much more rapid in the SCF.

The lifetime of  $e_s^-$  formed by photoinjection into pure supercritical ammonia (containing no added electrolyte) has been re-

ported to be around  $5 \mu\text{s}$ .<sup>28h</sup> Schindewolf et al.<sup>30</sup> chemically generated long-lived solutions of  $e_s^-$  in supercritical ammonia by forcing the equilibrium of eq 10 to the right, but this situation is not analogous to the electrochemical experiment, where there is no excess of  $\text{H}_2$  or  $\text{NH}_2^-$ .

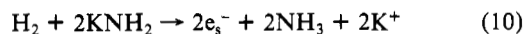


Figure 8 shows new voltammetric data obtained for the electrochemical generation of  $e_s^-$  in supercritical ammonia. The most noticeable features of this voltammetry, as compared to the previous experiments,<sup>2</sup> are the absence of a prewave just positive of the onset of  $e_s^-$  at temperatures above  $25 \text{ }^\circ\text{C}$  and a wave near 0 V at  $150 \text{ }^\circ\text{C}$ , which corresponds to the reoxidation of  $e_s^-$ . We now know the prewave to be due to the presence of trace water,<sup>31</sup>

(30) Schindewolf, U.; Vogelsang, R.; Bodeker, K. W. *Angew. Chem., Int. Ed. Engl.* 1967, 6, 1076–1077.

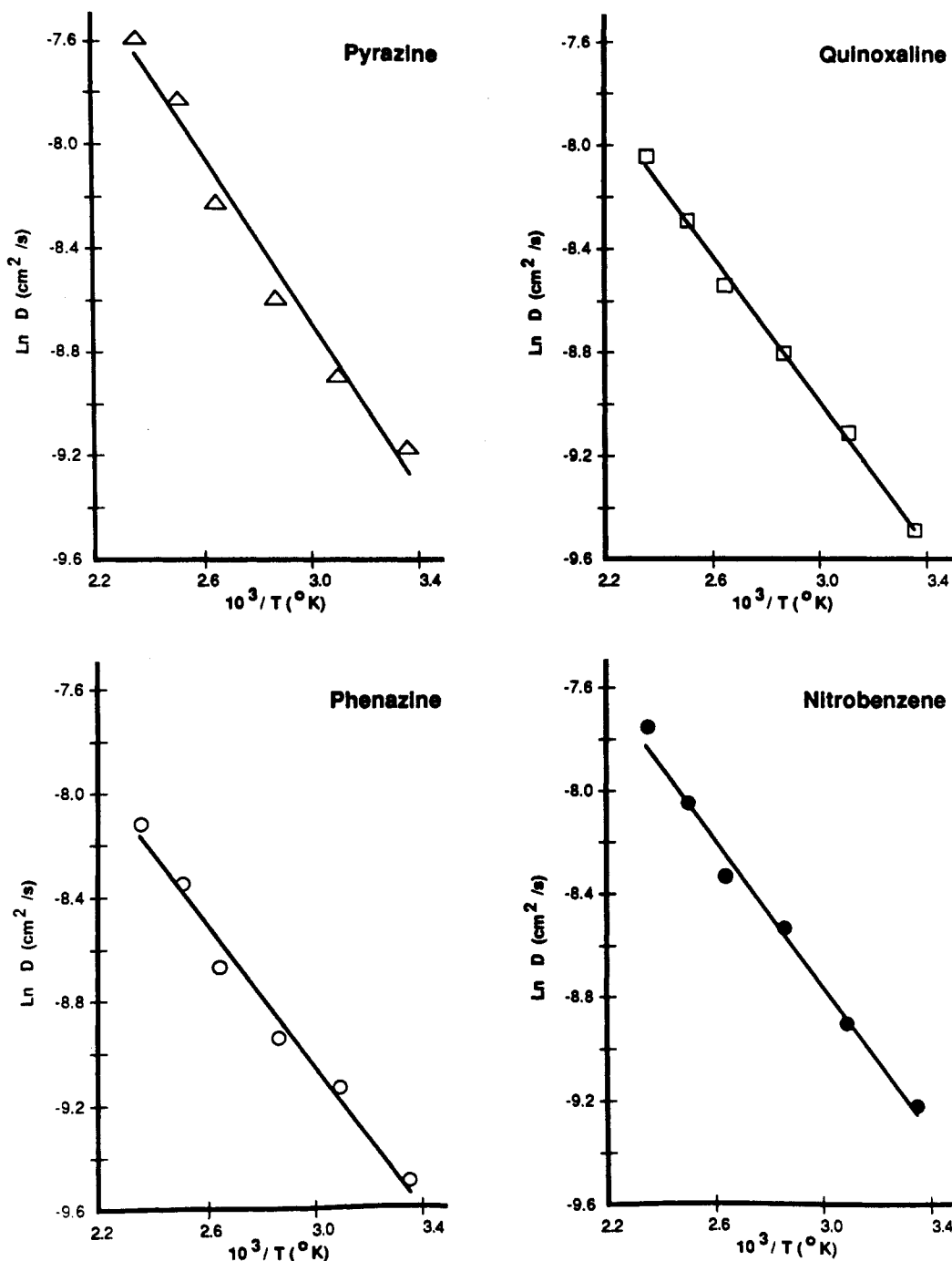


Figure 7. Plot of  $\ln D$  (diffusion coefficient) vs.  $1/T$ .

which might account for our initial failure to observe a current for the oxidation of  $e_s^-$ . Pure water is known to react very quickly with  $e_s^-$  ( $t_{1/2}$  ca. 100  $\mu$ s):<sup>32a</sup>



However, Schindewolf<sup>32b</sup> reported that the lifetime of  $e_s^-$  increased exponentially with increasing mole fraction of ammonia; for a 20% solution of water in ammonia,  $t_{1/2}$  for  $e_s^-$  is around 100 s. Therefore, in our system, reaction of  $e_s^-$  with water is probably very slow even at elevated temperature because of the extremely low level of water present. A second explanation involves the presence of electron traps generated in the working solution at

(31) (a) Herlem, M. *Bull. Soc. Chim. Fr.* **1967**, 1687. (b) Herlem, M.; Minet, J.; Thiebault, A. *J. Electroanal. Chem.* **1971**, *30*, 203.

(32) (a) Gould, R. F., Ed. *Advances in Chemistry*; American Chemical Society: Washington, D.C., 1965; Vol. 50. (b) Schindewolf, U. In *Metal-Ammonia Solutions*; Lagowski, J. J., Sienko, M. J., Eds.; Butterworths: London, 1970; pp 199–218.

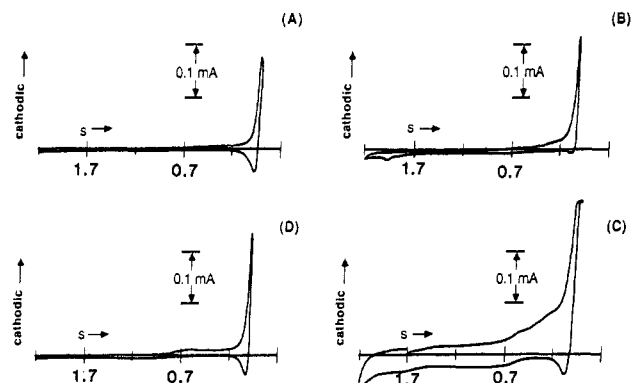


Figure 8. Cyclic voltammetry of solvated electrons ( $e_s^-$ ) in ammonia/ $\text{CF}_3\text{SO}_3\text{K}$ : (A) 25 °C, 9.5 bar, scan rate ( $\nu$ ) = 1 V/s; (B) 100 °C, 100 bar,  $\nu$  = 1 V/s; (C) 150 °C, 285 bar (supercritical),  $\nu$  = 10 V/s; (D) 25 °C (after cooling from 150 °C), 9.5 bar,  $\nu$  = 1 V/s. Potentials vs.  $e_s^-$ .

the counter electrode. For example,  $H^+$  in the form  $NH_4^+$  reacts rapidly with  $e_s^-$  ( $k = 4 \times 10^{-6} M^{-1} s^{-1}$  at  $-34^\circ C$ ):<sup>33</sup>



At present, we are unable to determine the rate-determining step for the disappearance of  $e_s^-$  in supercritical ammonia; however, from the sweep rate at which reoxidation of  $e_s^-$  is detectable at  $150^\circ C$  (Figure 8C), we estimate  $t_{1/2}$  of electrochemically generated  $e_s^-$  in supercritical ammonia containing electrolyte to be at least 5 ms. This figure represents a lower limit, because a trace of water or other reactive impurity may be present which affects the stability of  $e_s^-$ .

**Thermodynamics.** To relate potentials to one another, it is necessary to establish an arbitrary standard electrode. The normal hydrogen electrode (NHE) has been selected as the standard reference electrode, and the half-reaction which this electrode represents



is assigned a potential of 0 V at all temperatures in all solvents. The difficulty of building a NHE for use in a SCF has already been discussed. This prevents assignment of half-reaction potentials on the NHE scale but does not hinder thermodynamic measurement of the free energy change of chemical reactions,  $\Delta G_{rxn}$ , or  $\Delta S_{rxn}$  and  $\Delta H_{rxn}$  from the temperature coefficient of the potential. The derivative of potential with temperature at constant pressure yields the entropy change ( $\Delta S$ ) of a cell reaction

$$\Delta S = nF(dE/dT)_p \quad (14)$$

where  $n$  is the number of electrons involved in the reaction,  $F$  the Faraday, and  $E$  the potential of the reversible reaction. If all species involved in the reaction are in their standard states and if the diffusion and activity coefficients of the oxidized and reduced species taking part in the reaction are the same, then eq 14 can be rewritten

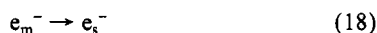
$$\Delta S^\circ = nF(dE_{1/2}/dT)_p \quad (15)$$

where  $E_{1/2}$  is the polarographic half-wave potential which is available from cyclic voltammetry.  $E_{1/2}$  was obtained from the average of  $E_{p,c}$  and  $E_{p,a}$  so that deviations because of  $iR$  drop and quasi-reversibility are minimized.

In Figure 9 the values of  $E_{1/2}$  are plotted against temperature for the first reductions of PYR, QUIN, PHEN, and NB and for the second reductions of QUIN and PHEN. The slopes of the linear portions of the resulting lines,  $dE_{1/2}/dT$ , are tabulated in Table II, along with the calculated value of  $\Delta S^\circ_{rxn}$ . For convenience many of the values of  $dE_{1/2}/dT$  were not acquired at constant pressure; however, those that were demonstrated the pressure effect on  $\Delta S$  to be negligible for these reactions over the pressure range 10–350 bar. The entropy values we report are for the reaction



which is comprised of the two half-reactions



where  $e_m^-$  is the electron in the metal electrode. The measured reaction entropy of eq 16 arises primarily from restructuring of the solvent around the radical anion and the solvation entropy of  $e_s^-$  (eq 18). The Born equation<sup>34</sup> can be used to estimate the difference in solvation entropy for a neutral species and its ion, essentially the reaction entropy of eq 17

$$\Delta S^\circ = z^2 e^2 N (\partial \epsilon / \partial T) / 8 \pi \epsilon_0 r \epsilon^2 \quad (19)$$

where  $z$  is the change on the ion,  $\epsilon_0$  the permittivity of free space,  $e$  the charge on the electron,  $r$  the radius of the ion,  $N$  Avogadro's number, and  $\epsilon$  the dielectric constant of the medium at the tem-

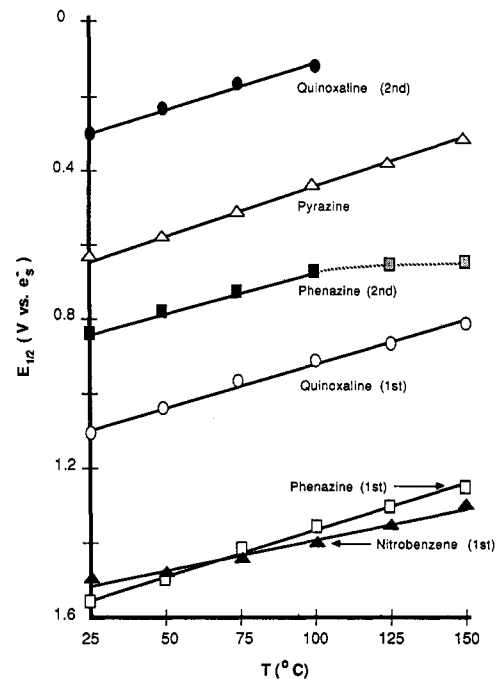


Figure 9. Dependence of the polarographic half-wave potential ( $E_{1/2}$ ) on temperature. 1st and 2nd refer to the first and second reductions as shown in eq 2 and 3.

perature of interest. If the radius of the ion is taken as the hydrodynamic radius (average  $r = 1.7 \text{ \AA}$ ) derived from the Stokes–Einstein relationship (eq 7) and  $\partial \epsilon / \partial T$  is taken from the literature,<sup>35</sup> then  $\Delta S^\circ$  at  $25^\circ C$  ranges from  $-140$  to  $-190 \text{ J/(K mol)}$  for the solvation of the ions studied. These theoretical values can be compared to the experimental results, if the solvation entropy of  $e_s^-$  (eq 18) is accounted for; that is

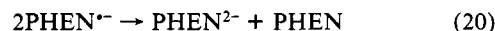
$$\Delta S^\circ_{eq 16} + \Delta S^\circ_{eq 18} = \Delta S^\circ_{eq 17}$$

where  $\Delta S^\circ_{eq 18} \sim 48 \text{ J/(K mol)}$ .<sup>36</sup> The average experimental value of  $\Delta S^\circ_{eq 17}$  is  $-172 \text{ J/(K mol)}$ , in good agreement with the average theoretical value,  $-165 \text{ J/(K mol)}$ .

Few entropy measurements for the reduction of aromatics in aprotic solvents have been made previously. Schindewolf<sup>37</sup> measured  $\Delta S_{rxn}$  for the reduction of nine aromatics in liquid ammonia by homogeneous reaction of the neutral species with  $e_s^-$  between  $-75$  and  $-35^\circ C$ .  $\Delta S_{rxn}$  was found to average  $-215 \pm 25 \text{ J/(K mol)}$ , in good agreement with the average of this study,  $\Delta S^\circ_{rxn} = -220 \pm 40 \text{ J/(K mol)}$ . Savéant<sup>38</sup> measured the relative difference in entropy between successive electron transfers for a series of polynitro compounds in aprotic solvents, but he did not report the change in entropy ( $\Delta S$ ) for individual reductions.

An additional interesting feature of Figure 9 is that the  $E_{1/2}$  vs.  $T$  lines are straight, except in one case, indicating no temperature dependence on the entropy even in the SCF. This suggests that the change in solvent organization between the  $R/R^{\cdot-}$  and  $R^{\cdot-}/R^{2-}$  couples in liquid and supercritical ammonia is generally quite similar; however, the aberrant behavior of the second reduction of PHEN may indicate a change in the nature of the solvation upon reduction of  $PHEN^{\cdot-}$  at low and high temperature.

The thermodynamic parameters  $\Delta G^\circ_{rxn}$ ,  $\Delta S^\circ_{rxn}$ , and  $\Delta H^\circ_{rxn}$  for the cross-reactions between any of the neutral, anionic, or dianionic species investigated can be calculated from the data in Table II. For example, the equilibrium constant,  $K$ , for the disproportionation of  $PHEN^{\cdot-}$



(35) Reference 4a, p 243.

(36) Lepoutre, G.; Jortner, J. *J. Phys. Chem.* **1972**, *76*, 683–687.

(37) Gross, W.; Schindewolf, U. *Ber. Bunsenges. Phys. Chem.* **1981**, *85*, 112–116.

(38) (a) Ammar, F.; Savéant, J. M. *J. Electroanal. Chem.* **1973**, *47*, 115–125. (b) Andrieux, C. P.; Savéant, J. M. *J. Electroanal. Chem.* **1974**, *57*, 27–33.

(33) Schindewolf, U. *J. Phys. Chem.* **1984**, *88*, 3820–3826.

(34) Lewis, G. N.; Randall, M. *Thermodynamics*, 2nd ed.; McGraw-Hill: New York, 1961; p 523.

can be calculated at any temperature since

$$\Delta E_{p,c} = RT/nF \ln K \quad (21)$$

where  $\Delta E_{p,c}$  is the difference in potential for the reductions of PHEN and PHEN<sup>•-</sup>. For eq 20 at 25 and 150 °C,  $K = 9.2 \times 10^{-13}$  and  $2.1 \times 10^{-11}$ , respectively.

### Conclusions

We have demonstrated that normal electrochemical techniques are applicable to supercritical ammonia solutions, although the implementation can be somewhat challenging. Aside from an increase in solution resistance, the results of cyclic voltammetric and chronoamperometric experiments indicate that electrochemical processes that are reversible in liquid ammonia at low temperature are reversible, or nearly reversible, in the SCF. The behavior of PHEN in the SCF was found to be analogous to that at -40 °C, indicating that the intrinsic nature of ammonia, rather than lowered temperature, is responsible for the stability of the dianion. The chemistry of following homogeneous reactions of NB in the SCF was interpreted in terms of results obtained at low temperature, thereby demonstrating the functional similarity of liquid and supercritical ammonia. Further work on the kinetics of coupled homogeneous reactions and heterogeneous electron transfer is anticipated.

The standard potentials of all redox couples studied became more negative with an increase in temperature, indicating increased solvation (and ion pairing) upon reduction. Since this change was

generally linear throughout the temperature range studied, the nature of solvation between liquid ammonia and the SCF is not very different. Overall, the experimental results show that free energies of reaction and other thermodynamically meaningful parameters are accessible from electrochemical experiments in the SCF.

Diffusion coefficients, determined for temperatures up to 150 °C, demonstrated that the hydrodynamic Stokes-Einstein relationship, and the theory of activated diffusion, can be applied to the SCF. Such agreement suggests that many of the concepts that underlie solvation of normal liquids also apply to the SCF. Thus, electrochemistry is a valuable probe of species in the supercritical phase and is quite similar to that found at lower temperatures. It should be possible to take advantage of the tunable parameters of the SCF, such as the solvating power, to perform new types of syntheses and separations. Electrochemistry should also be a valuable tool for understanding the structure of the supercritical state.

*Acknowledgment.* The support of this research by the Office of Naval Research and the Separations Research Program at the University of Texas is gratefully acknowledged. We also thank Ramy Farid for his assistance during initial experiments.

**Registry No.** NB, 98-95-3; NB<sup>•-</sup>, 12169-65-2; NB<sup>2-</sup>, 56939-13-0; PYR, 290-37-9; PYR<sup>•-</sup>, 34512-20-4; QUIN, 91-19-0; QUIN<sup>•-</sup>, 34504-55-7; QUIN<sup>2-</sup>, 106401-80-3; PHEN, 92-82-0; PHEN<sup>•-</sup>, 34467-89-5; PHEN<sup>2-</sup>, 106401-81-4; W, 7664-41-7; NH<sub>3</sub>, 2926-27-4; F<sub>3</sub>CSO<sub>3</sub>K, 2926-27-4.